Available online at www.sciencedirect.com
SCIENCE DIRECT®
Journal of Solid State Chemistry 178 (2005) 234–244
JOURNAL OF SOLID STATE CHEMISTRY
www.elsevier.com/locate/jssc

Energetics of $La_{1-x}A_xCrO_{3-\delta}$ perovskites (A = Ca or Sr)

Jihong Cheng, Alexandra Navrotsky*

Thermochemistry Facility and NEAT ORU, University of California at Davis, One Shields Avenue, Davis, CA 95616, USA

Received 24 August 2004; received in revised form 17 November 2004; accepted 26 November 2004

Abstract

A series of perovskites with the general formula $La_{1-x}A_xCrO_{3-\delta}$ (A = Ca or Sr) have been synthesized in the solid solution range $0.0 < x \leqslant 0.3$ and $0.0 \leqslant \delta \leqslant 0.5x$ with a variety of heat treatments. High-temperature drop solution calorimetry in molten $2PbO \cdot B_2O_3$ at 1080 K was performed to determine their enthalpies of formation from oxides at room temperature. The enthalpy of oxidation involved in the reaction $2Cr^{x}_{Cr} + V^{\cdot\cdot}_{O} + 0.5O_2(g) = 2Cr^{\cdot}_{Cr} + O^{x}_{O}$ is roughly independent of oxygen nonstoichiometry (δ) in each series with a given dopant composition, but varies with composition (x). The values change from -620 ± 260 to -280 ± 80 kJ/mol O_2 when $x = 0.1$–0.3 for Ca-doped samples, and from -440 ± 150 to -290 ± 50 kJ/mol O_2 for Sr-doped ones. This dependence of enthalpy of oxidation on composition suggests oxygen vacancies are increasingly short-range ordered in reduced samples. The higher oxidation state of chromium is stabilized by the substitution of alkaline earth ions, but with increasing doping, the enthalpy of formation of the fully oxidized sample in both Ca and Sr-doped systems becomes more endothermic. This destabilization effect is attributed to the large endothermic enthalpy of oxygen vacancy formation (395 ± 30 kJ/mol of $V^{\cdot\cdot}_{O}$) for the reaction $A^{x}_{A} + O^{x}_{O} = A^{'}_{La} + 0.5V^{\cdot\cdot}_{O} + 0.5O_2$(A = Ca or Sr) that over-rides the exothermic enthalpies of oxidation. At a given composition, Sr-doped $LaCrO_3$ is more stable than its Ca-doped counterpart, which is consistent with basicity arguments.

Keywords: Enthalpy of formation; Thermodynamics; Oxygen vacancies; Enthalpy of oxidation; Doped lanthanum chromite; Perovskites; Solid oxide fuel cells; Interconnect

1. Introduction

Solid oxide fuel cells (SOFCs) are promising power generation devices for more efficient and cleaner energy [1]. The interconnect in SOFCs serves as an electrical contact between individual cells and, additionally, separates the gas compartments in planar systems. A number of requirements need to be satisfied for a good interconnect material at the fuel cell operating temperature (~1273 K): high and purely electronic conductivity, good thermal stability in both reducing and oxidizing atmospheres, good thermal compatibility with adjacent components (anode and cathode), and matched thermal expansion with other components. Alkaline earth (Mg, Ca, or Sr) doped $LaCrO_3$ perovskites have been almost the exclusive choice for decades because they meet most of these criteria [1,2].

Undoped $LaCrO_3$ is a very refractory ceramic oxide and shows p-type conduction due to electron holes in the *3*d band of the chromium ions [1]. Upon the substitution of alkaline earth cations, e.g., A^{2+} for La^{3+} (A = Ca or Sr), the difference in ionic charge between the dopant and host must be compensated. Two scenarios are possible depending on the oxygen partial pressure and temperature: oxidation of the transition metal (chromium) in the structure, or creation of oxygen vacancies on the oxygen sublattice. A point defect model has been widely used to describe the defect structure, e.g., in the case of Sr doping by Mizusaki et al. [3], Ca doping by Yasuda and Hikita [4], and multiple-cation doping by Zuev et al. [5]. For a $La_{1-x}A_xCrO_{3-\delta}$ system ($0 \leqslant \delta \leqslant x/2$), the major defects involved are $A^{'}_{La}$ (dopant), $V^{\cdot\cdot}_{O}$ (oxygen vacancy), and$Cr^{\cdot}_{Cr}$ (formal

*Corresponding author. Fax: 530 752 9307.
E-mail address: anavrotsky@ucdavis.edu (A. Navrotsky).

0022-4596/$ - see front matter © 2004 Elsevier Inc. All rights reserved.
doi:10.1016/j.jssc.2004.11.028

Cr^{4+}), and the defect chemistry is represented by Eqs. (1) and (2) (Kröger–Vink notation is taken [6])

$$A_A^x + Cr_{Cr}^x = A'_{La} + Cr_{Cr}^{\cdot} \quad (1)$$

$$2Cr_{Cr}^{\cdot} + O_O^x = 2Cr_{Cr}^x + V_O^{\cdot\cdot} + 0.5O_2. \quad (2)$$

The variation in defect chemistry, i.e., the interplay between the redox of Cr and the creation-disappearance of oxygen vacancies, has profound effects on the performance of SOFCs. Under oxidizing conditions, where the interconnect is near the cathode side in SOFCs, the charge compensation is primarily electronic (Eq. (1)) and oxygen vacancies are negligible ($\delta \approx 0$). Doping introduces additional electron holes and thus substantially enhances the electronic conduction through a small polaron hopping mechanism between Cr^{3+} and Cr^{4+} [7]. Near the anode side which is strongly reducing, ionic charge compensation becomes significant via the formation of oxygen vacancies (Eq. (2), $\delta > 0$), causing an appreciable decrease of the electronic conductivity [8]. A conductivity gradient is thus expected to exist across the interconnect. Fortunately, the overall electronic conductivity of doped $LaCrO_3$ is still adequate for its use [9].

Thermal expansion of the interconnect is potentially another issue. Undoped $LaCrO_3$ undergoes a structural phase transition from orthorhombic to rhombohedral around 533 K accompanied by a volume shrinkage [10]. Doping with different species (Ca or Sr) and amounts (0–30 mol%) modifies the thermal expansion coefficient and phase transition characteristics, and therefore may cause thermal expansion mismatch with neighboring components [11,12]. Furthermore, thermal expansion varies greatly with oxygen nonstoichiometry. Exposure to reducing atmospheres results in the formation of oxygen vacancies at the cost of Cr^{4+}. The lattice is expanded due to the reduced coulombic attraction between cations and anions and the simultaneous reduction of Cr^{4+} to the larger Cr^{3+} [4,13]. The expansion, if severe enough, may lead to undesirable swelling [2].

Thermodynamic data are of critical importance to evaluate and predict the stability and compatibility of components at the fuel cell operating temperature. Since properties such as catalysis and electrical conductivity are closely related to the coexistence of variable oxidation states of the transition metal, the redox energetics between different formal oxidation states (Cr^{3+} and Cr^{4+} in this case) is of great importance and several techniques have been developed to study the redox thermodynamics. Most often, oxygen nonstoichiometry is established, either from thermogravimetry (TG) [3] or from electrical conductivity measurement [4], as a function of the oxygen partial pressure in a given temperature range. The enthalpy and entropy can be deduced from the temperature dependence of the defect equilibria [3,4]. Alternatively, direct determination of the enthalpy of oxidation is possible. Stølen et al. [14,15] recently applied high-temperature adiabatic calorimetry as a new approach to study the redox thermochemistry. High-temperature oxide melt solution calorimetry [16,17] is another versatile tool to measure the heat of oxidation and has been applied to various perovskite-related systems [18–21]. The latest study using solution calorimetry was on the Sr-doped $LaFeO_3$ system [22]. Studies of other thermodynamic quantities such as enthalpy of formation, however, are rather limited.

We have successfully applied high-temperature solution calorimetry to study the enthalpy of formation of the end-member $LaCrO_3$ along with other perovskites $LaMO_3$ (M = Fe, Co, and Ni) [23]. In the current work, a suite of $La_{1-x}A_xCrO_{3-\delta}$ samples (A = Ca or Sr, $x \leqslant 0.3$) was synthesized with oxygen contents in the range of $0.0 \leqslant \delta \leqslant 0.5x$. We report their enthalpies of formation from oxides and explore the energetic trends throughout the solid solution in terms of dopant species and doping amount. The enthalpy of oxidation of Cr^{3+} to formal Cr^{4+} is determined for each Ca/Sr composition and compared to values available in the literature.

2. Experimental

2.1. Synthesis and characterization

Ca-doped $LaCrO_3$ (LCC) and Sr-doped $LaCrO_3$ (LSC) perovskites ($0.0 < x \leqslant 0.3$, and $0.0 \leqslant \delta \leqslant 0.5x$) were first synthesized by either a solid-state reaction (SSR) method or a sol–gel method [23]. A portion of each sample was subsequently subjected to further heat treatment to generate additional samples with different δ values. A summary of all 12 samples and their detailed synthesis or heat treatment parameters are listed in Table 1. Each sample, generally written as $La_{1-x}A_xCrO_{3-\delta}$ (A = Ca or Sr), is conveniently denoted by a combination of its dopant composition and oxygen content. For instance, for 20 mol% Sr-doped $LaCrO_3$ with oxygen deficiency of 0.09, the sample is coded as L20SC2.91.

The conventional SSR method started with La_2O_3, Cr_2O_3 and $CaCO_3$ or $SrCO_3$ (purity > 99.99%, La_2O_3 from Aldrich, others from Alfa Æsar). As-received La_2O_3 powder was dried under vacuum at 1073 K and weighed in an Ar-filled glovebox. Powders with the proper cation ratio were mixed thoroughly in an alumina mortar and pressed into discs for pre-calcination at 1273 K for 12 h. The heat-treated discs were then crushed and ground. The powder was pelletized under a uniaxial pressure of 25 MPa and was sintered in air at 1773 K. The alumina boat which contained the sample pellets was coved with platinum foil to avoid possible reactions between $LaCrO_3$ and Al_2O_3 at high

Table 1
Synthesis, phase identification, and chemical analysis of $La_{1-x}A_xCrO_{3-\delta}$ samples (A = Ca or Sr)

	X	Sample code	$3-\delta$[a]	Total cation weight %[b]		Structure[c]	Synthesis/treatment conditions
				Nominal	Measured		
Ca-doped	0.1	L10CC3.0	3.00	79.04	79.13±0.54	O	SSR or sol–gel, sintered at 1773 K in air
		L10CC2.98	2.98			O	From L10CC3.0, TG in 1% H_2 to 1273 K, 1 h
	0.2	L20CC3.0	3.00	78.10	77.83±0.55	O	SSR or sol–gel, sintered at 1773 K in air
		L20CC2.93	2.93			O	From L20CC3.0, TG in 1% H_2 to 1273 K, 1 h
	0.3	L30CC3.0	3.00	77.06	76.82±0.59	O	SSR or sol–gel, sintered at 1773 K in air
		L30CC2.91	2.91			O	From L30CC3.0, TG in 1% H_2 to 1273 K, 1 h
Sr-doped	0.1	L10SC3.0	3.00	79.47	79.40±1.08	R	SSR, annealed at 1773 K in O_2
		L10SC2.96	2.96			R	From L10SC3.0, TG in 1% H_2 to 1273 K, 1 h
	0.2	L20SC3.0	3.00	79.01	79.00±0.64	R	SSR, annealed at 1773 K in O_2
		L20SC2.91	2.91			R	From L20SC3.0, TG in 1% H_2 to 1273 K, 1 h
	0.3	L30SC3.0	3.00	78.53	78.39±1.04	R	SSR, annealed at 1773 K in O_2
		L30SC2.89	2.89			R	From L30SC3.0, TG in 1% H_2 to 1273 K, 1 h

[a]Fully oxidized samples were verified by electron microprobe analysis. Oxygen content in reduced samples was determined from TG measurement and the uncertainty is estimated as ±0.01.
[b]The calculations of the total cation weight % were all based on fully oxidized samples, i.e., $\delta = 0$. The measured values (microprobe) agree well with the nominal ones.
[c]O = orthorhombic, R = rhombohedral.

temperatures. All samples were furnace cooled to room temperature. Grinding, pelletizing and sintering were repeated to ensure complete reaction.

LSC samples synthesized in air were reported to contain two perovskite-like phases, one orthorhombic and the other rhombohedral [24,25], but annealing in pure oxygen can help convert the sample to a single rhombohedral phase [24]. Therefore, the three LSC samples were annealed in O_2 at 1773 K for 50 h with several intermediate grindings (Table 1).

LCC powders synthesized by SSR were found to be difficult to pelletize for drop solution (DS) calorimetry. Alternatively, the low-temperature sol–gel method was attempted, which started with lanthanum acetate, calcium acetate, and chromium nitrate (purity > 99.99%, all from Alfa Æsar). For each LCC sample, appropriate amounts of the starting chemicals were dissolved in 200 mL of deionized water with vigorous stirring. The clear solution was peptized by adding ammonia to form a gel with pH = 10. The resulting gel was dried in a box oven at 423 K for 8 h, followed by a pre-calcination at 973 K overnight. The powder obtained was pelletized under 25 MPa and finally sintered at 1723 K for 1 day in air.

To obtain doped $LaCrO_3$ with large oxygen deficiency, an in situ TG method similar to the syntheses of $La_{1-x}Sr_xFeO_{3-\delta}$ [22] was used. Oxygen nonstoichiometry is a function of the oxygen partial pressure and temperature, which can be well controlled in a TG apparatus. TG coupled with differential scanning calorimetry (DSC) was performed on a Netzsch STA 449 from room temperature to 1273 K. Analyses were conducted using the software supplied by the manufacturer after continuous runs of the baseline and sample. About 80 mg of sample prepared under ambient conditions (LCC) or in pure O_2 (LSC) was pelletized to ensure good thermal contact with the Pt crucible and was heated at 10 K/min in a specified atmosphere with a flow rate of 40 mL/min. Unlike Sr-doped $LaFeO_3$ [22], all chromite samples were stable in Ar to 1273 K. A gas mixture of 1% H_2 and 99% Ar was effective to increase δ at 1273 K. The total weight loss, except that from a small amount of surface water which desorbed below 450 K, was assigned to the oxygen reduction. A new formula for the sample after TG was calculated. The accuracy and usefulness of this TG treatment method have been addressed in the study of the $La_{1-x}Sr_xFeO_{3-\delta}$ system [22]. Some of the reduced samples were treated in O_2 with TG/DSC to measure the weight gain and the enthalpy of oxidation. The heating rate was 20 K/min and the temperature range was 298–1173 K, with a 1 h isotherm at 1173 K.

Phase identification was carried out by powder X-ray diffraction (XRD) using a Scintag PAD V diffractometer (Cu$K\alpha$ radiation) operated at 45 kV and 40 mA, with a 0.02° step size and 2–10 s dwell time.

A Cameca SX-100 electron microprobe was used for chemical analysis. Sample homogeneity was examined qualitatively by X-ray dot mapping and back-scattered electron images, while quantitative chemical analysis was determined by wavelength-dispersive spectroscopy (WDS). $LaPO_4$, $CaWO_4$, $SrTiO_3$, and Cr_2O_3 were used as standards for La, Ca, Sr, and Cr, respectively. It is worth noting that using chromium metal as the standard for Cr in doped $LaCrO_3$ led to a significantly nonstoichiometric cation ratio. Using Cr_2O_3 gave much

better results, presumably because of its similar bonding than in $LaCrO_3$ perovskites. A direct and accurate measurement of oxygen is difficult and time consuming due to the severe interference between the characteristic X-ray peaks of oxygen and chromium. However, the cation ratios obtained by microprobe are reliable and the oxygen content can be indirectly verified.

2.2. High-temperature oxide melt solution calorimetry

High-temperature DS calorimetry was performed for all doped chromite samples in a Tian–Calvet twin microcalorimeter using lead borate ($2PbO \cdot B_2O_3$) as the solvent at 1080 K. Details of the equipment and experimental procedures have been described elsewhere [16,17]. Calibration of the calorimeter was based on the heat content of ~5 mg corundum pellets as a standard laboratory protocol. Argon was flushed through the calorimeter assembly (40 mL/min) to expel any gas species evolved in the calorimeter. The solvent was agitated by bubbling argon gas through it (5 mL/min) to facilitate dissolution and prevent local saturation.

A reproducible final oxidation state of the chromium dissolved in the lead borate solvent is crucial to interpreting the calorimetric data. We have recently confirmed that Cr^{3+} is stable in lead borate under Ar atmosphere and Cr^{3+}-containing samples dissolves at a satisfactory rate at 1080 K [23]. Any formal Cr^{4+} in doped $LaCrO_3$ will be reduced to Cr^{3+} upon dissolution and released oxygen gas removed by dynamic Ar bubbling. Particular care was paid to the small amount of residual oxygen in the solvent before performing calorimetry. In preliminary DS experiments on Cr_2O_3, it was found that the first drop in any given batch of solvent invariably gave a different enthalpy of DS from the second and subsequent drops, which were consistent. We concluded that the inconsistency was due to the oxidation of Cr^{3+} to Cr^{6+} by residual oxygen in the melt during the first dissolution [23]. Therefore, some Cr_2O_3 was intentionally dropped into the solvent to consume the residual oxygen during the time the calorimeter was reaching thermal equilibrium. The following drops of other samples of interest gave statistically consistent values.

DS calorimetry involves dropping a sample pellet from room temperature (298 K) into the molten solvent in the calorimeter at 1080 K. For samples with virtually no Cr^{4+} present, the total heat effect, enthalpy of DS (H_{DS}), is equal to the heat of solution at 1080 K plus the heat content from 298 to 1080 K. For samples containing Cr^{4+}, the heat effect associated with the reduction of Cr^{4+} to Cr^{3+} is included in the enthalpy of DS.

CaO and SrO are too hygroscopic to be prepared and handled easily. Their enthalpies of DS were calculated from the enthalpies of DS of $CaCO_3$ and $SrCO_3$ and other related thermodynamic data using the first thermochemical cycle in Table 2. The enthalpies of formation from oxides for the $La_{1-x}A_xCrO_{3-\delta}$ samples

Table 2
Thermochemical cycles for calculation of the enthalpy of drop solution of AO in $2PbO \cdot B_2O_3$ at 1080 K (cycle 1) and the enthalpies of formation from oxides for $La_{1-x}A_xCrO_{3-\delta}$ perovskites (cycle 2) at room temperature (A = Ca or Sr)

Reaction	ΔH
Cycle 1: Enthalpy of drop solution of AO	
ACO_3(xl, 298 K) → AO(sol, 1080 K) + CO_2(g, 1080 K)[a]	$\Delta H(1) = \Delta H_{DS}(ACO_3)$
CO_2(g, 298 K) → CO_2(g, 1080 K)	$\Delta H(2) = \Delta H_{298-1080}(CO_2)$[b]
AO(xl, 298 K) + CO_2(g, 298 K) → ACO_3(xl, 1080 K)	$\Delta H(3) = \Delta H^{\circ}_{f,ox}(ACO_3)$[c]
AO(xl, 298 K) → AO(sol, 1080 K)	
$\Delta H(4) = \Delta H(1) - \Delta H(2) + \Delta H(3)$	$\Delta H(4) = \Delta H_{DS}(AO)$
Cycle 2: Enthalpy of formation of $La_{1-x}A_xCrO_{3-\delta}$ from oxides	
La_2O_3(xl, 298 K) → La_2O_3(sol, 1080 K)	$\Delta H(5) = \Delta H_{DS}(La_2O_3)$
Cr_2O_3(xl, 298 K) → Cr_2O_3(sol, 1080 K)	$\Delta H(6) = \Delta H_{DS}(Cr_2O_3)$
AO(xl, 298 K) → AO(sol, 1080 K)	$\Delta H(4) = \Delta H_{DS}(AO)$
O_2(g, 298 K) → O_2(g, 1080 K)	$\Delta H(7) = \Delta H_{298-1080}(O_2)$[d]
$La_{1-x}A_xCrO_{3-\delta}$(xl, 298 K) → $0.5(1-x)La_2O_3$(sol, 1080 K) + $0.5\,Cr_2O_3$(sol, 1080 K) + $x\,AO$(sol, 1080 K) + $(0.25x - 0.5\delta)\,O_2$(g, 1080 K)	$\Delta H(8) = \Delta H_{DS}(La_{1-x}A_xCrO_{3-\delta})$
$0.5(1-x)La_2O_3$(xl, 298 K) + $0.5\,Cr_2O_3$(xl, 298 K) + xAO(xl, 298 K) + $(0.25x - 0.5\delta)\,O_2$(g, 298 K) → $La_{1-x}A_xCrO_{3-\delta}$(xl, 298 K)	
$\Delta H(9) = 0.5(1-x)\,\Delta H(5) + 0.5\,\Delta H(6) + x\,\Delta H(4) + (0.25x - 0.5\delta)\,\Delta H(7) - \Delta H(8)$	$\Delta H(9) = \Delta H^{\circ}_{f,ox}\,(La_{1-x}A_xCrO_{3-\delta})$

[a] xl = crystalline solid, g = gas; sol = solution in $2PbO \cdot B_2O_3$.
[b] Heat content of CO_2 from 298 to 1080 K, calculated from Robie and Hemingway [26], 37.79 kJ/mol.
[c] Enthalpy of formation of ACO_3 from oxides at 298 K, calculated from Robie and Hemingway [26], -178.80 ± 1.58 kJ/mol for $CaCO_3$ and -233.90 ± 1.81 kJ/mol for $SrCO_3$.
[d] Heat content of O_2 from 298 to 1080 K, calculated from Robie and Hemingway [26], 25.50 kJ/mol.

($A = Ca$ or Sr) were calculated using the second thermochemical cycle in Table 2.

3. Results and discussion

3.1. Sample synthesis and characterization

Ca-doped $LaCrO_3$ samples, prepared either by SSR or sol–gel methods, were confirmed to be single phase with orthorhombic perovskite-type structure by powder XRD, consistent with other structural studies [4,27,28]. However, X-ray dot mapping and back-scattered electron images showed that SSR samples had local Ca-rich and Ca-poor regions at micron resolution. Homogeneity was improved with more grinding and firing and finally reached the same level as sol–gel samples.

Sr-doped $LaCrO_3$ samples, before annealing in O_2, consisted of two perovskite-type phases, rhombohedral in majority and some orthorhombic, which was also reported by Khattak and Cox [24]. A number of cycles of grinding and annealing in O_2 ensured each LSC sample was homogeneous and single phase with rhombohedral structure (Table 1).

Doped chromite perovskites obtained under oxidizing conditions (in air or O_2) have proven to be essentially fully oxidized ($\delta \approx 0$) by numerous studies, including potentiometric titration [13] and TG [3,5,24,28]. The stoichiometry was verified in this study by chemical analysis with WDS. The cation ratio in each sample was found to be close to the nominal one and only the total cation weight percentage is listed in Table 1. Assuming the oxygen content in each sample is 3.0, the theoretical total cation weight percentage is calculated. As seen from Table 1, the experimental values agree well with the calculated ones. Actually, Sakai et al. [14,28] have reported that oxygen-deficient LCC samples are metastable in air at room temperature and tend to gain oxygen given enough time.

Electron microprobe analysis also showed the importance of using Pt foil to separate the sample and Al_2O_3 boat during sintering at 1773 K because observable amount of Al diffused into those samples which directly contacted the container.

The oxygen content in each doped chromite sample, $3–\delta$, depends on the doping level of Sr, oxygen partial pressure and annealing temperature (Table 1). Using TG, oxygen nonstoichiometry analyses were coupled with the syntheses of oxygen-deficient samples in reducing atmospheres ($1\%H_2$). Under the same conditions, Ca-doped samples tend to retain more oxygen than their Sr-doped counterparts. Examples of TG/DSC curves are shown in Fig. 1. The TG results in Fig. 1 (a) show that three fully oxidized LCC samples, when treated in 1% H_2 at 1273 K for 1 h, lost weight to become L10CC2.98, L20CC2.93, and L30CC2.91, respectively. Fig. 1(b)–(d) illustrate the reoxidation behavior of three reduced samples, L10SC2.96, L20SC2.91, and L30CC2.91, respectively. Samples were treated in O_2 at 20 K/min to 1173 K with 1 h isotherm (not shown). The final weight gain in each case corresponds to the amount of oxygen needed to oxidize the sample to stoichiometry ($\delta = 0-0.01$). Oxygen absorption starts quickly around 400 K and ends at 600–750 K depending on the oxygen deficiency in each sample. Fig. 1(b)–(c) indicates that oxidation is exothermic and the area under each DSC peak represents the enthalpy of oxidation.

DSC is sensitive to detect phase transitions if their heat effect is larger than the sensitivity [29,30]. The small endothermic peak around 729 K in Fig. 1(d) indicates the structural phase transition of L30CC3.0 from orthorhombic to rhombohedral. Undoped $LaCrO_3$ is orthorhombic at room temperature and transforms to rhombohedral at 533 K [10]. Doping with Ca^{2+} shortens the average A–O bond length because the radius of Ca^{2+} is smaller than that of the host La^{3+} [31]. Thus more distortion is expected in the structures of LCC perovskites. Sakai and Stølen [27] measured the heat capacities of 10, 20, and 30 mol% Ca-doped $LaCrO_3$ using adiabatic calorimetry and reported the O to R phase transition temperatures as 568, 629, and 722 K, respectively. The transition point of L30CC in this study, 729 K, agrees well with theirs. On the other hand, doping with Sr^{2+} increases the average A–O bond length due to the larger radius of Sr^{2+} [31]. LSC samples are rhombohedral at room temperature, and therefore no phase transitions are observed (Fig. 1(b) and (c)).

In this study, we did not pursue the refinement of structures, but instead, highlight the effects of defect chemistry on the thermodynamic properties. This approach was also used in other thermodynamic studies [3,4]. The effect of these symmetry changes on the energetics is probably small (<1 kJ/mol) as seen for other perovskites [29,30].

3.2. Enthalpies of formation from oxides

The enthalpies of DS of constituent oxides (La_2O_3, Cr_2O_3, and AO) and $La_{1-x}A_xCrO_{3-\delta}$ samples ($A = Ca$ or Sr) and the corresponding enthalpies of formation from oxides at room temperature are summarized in Table 3. The exothermic formation enthalpies show the stability of each sample with respect to its component oxides.

The overall energetic trend in the $La_{1-x}A_xCrO_{3-\delta}$ system can be modeled by several competing factors including coupled substitution involving oxygen vacancy formation, short-range oxygen vacancy ordering, enthalpy of oxidation, and the chemical nature of

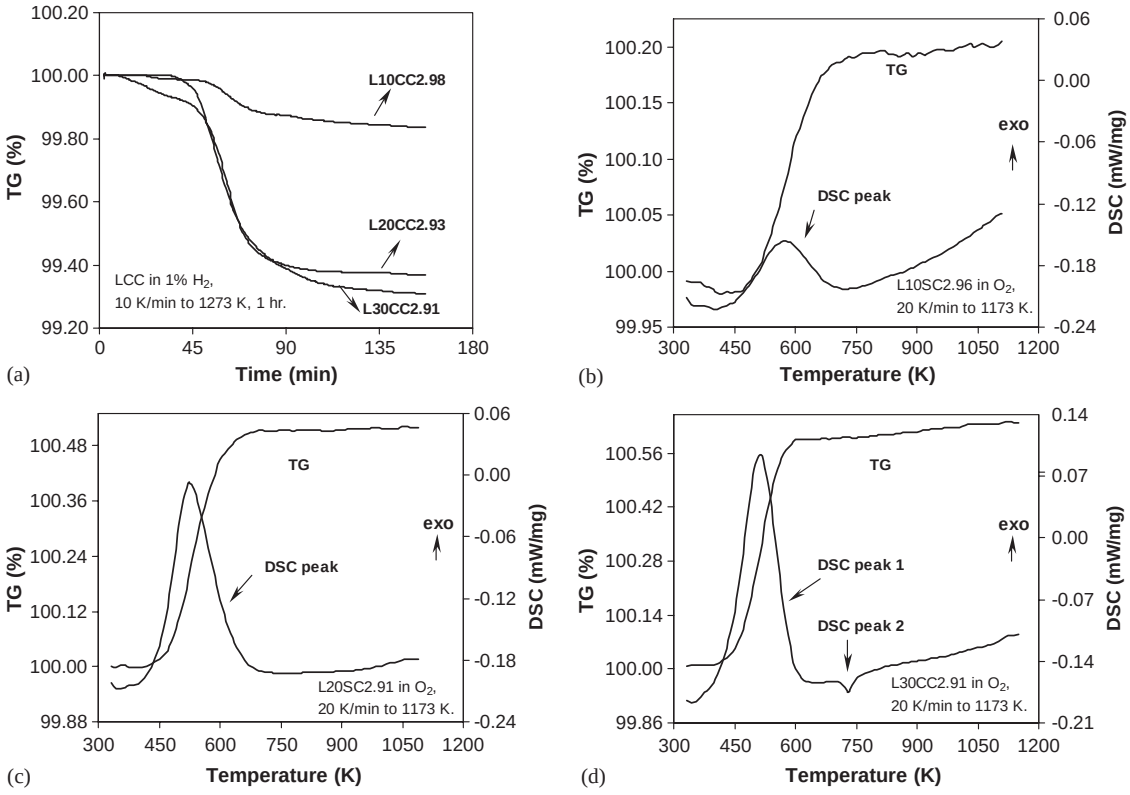

Fig. 1. TG/DSC curves of selected $La_{1-x}A_xCrO_{3-\delta}$ samples ($0.0 < x < 0.3$ and $0 \leqslant \delta < x/2$) indicating oxygen nonstoichiometry is a function of oxygen partial pressure and temperature. (a) Fully oxidized LCC perovskites were largely reduced in 1% H_2 at 1273 K for 1 h; (b), (c), and (d) examples of reoxidation for reduced samples L10SC2.96, L20SC2.91, and L30CC2.91, respectively. Samples were heated in O_2 at 20 K/min to 1173 K with 1 h isotherm. Isothermal sections are not shown.

Table 3
Enthalpies of drop solution (ΔH_{DS}) of oxides and $La_{1-x}A_xCrO_{3-\delta}$ perovskites (A = Ca or Sr) in $2PbO \cdot B_2O_3$ at 1080 K and enthalpies of formation of perovskites from oxides ($\Delta H_{f,ox}$) at room temperature

Sample	ΔH_{DS} (kJ/mol)	Sample	ΔH_{DS} (kJ/mol)	$\Delta H_{f,ox}$ (kJ/mol)
La_2O_3	-29.30 ± 4.43[a]	L10CC3.0	108.77 ± 1.57 (12)	-63.50 ± 2.24
Cr_2O_3	117.06 ± 0.57[b]	L10CC2.98	102.31 ± 2.08 (7)	-57.29 ± 2.65
$CaCO_3$	209.51 ± 1.64 (13)[c]	L20CC3.0	73.38 ± 1.63 (10)	-26.71 ± 2.31
$SrCO_3$	226.76 ± 2.35 (8)	L20CC2.93	61.36 ± 2.35 (7)	-15.59 ± 2.87
CaO	-7.08 ± 2.31	L30CC3.0	64.04 ± 1.34 (8)	-15.98 ± 2.12
SrO	-44.93 ± 2.99	L30CC2.91	50.47 ± 2.43 (6)	-3.55 ± 2.94
		L10SC3.0	109.37 ± 2.87 (10)	-67.88 ± 3.40
		L10SC2.96	100.13 ± 0.99 (9)	-59.15 ± 2.06
		L20SC3.0	89.64 ± 1.32 (16)	-50.54 ± 2.24
		L20SC2.91	72.71 ± 2.26 (10)	-34.76 ± 2.89
		L30SC3.0	73.43 ± 1.14 (15)	-36.72 ± 2.14
		L30SC2.89	55.78 ± 2.62 (9)	-20.48 ± 3.19

[a]From Cheng and Navrotsky [29].
[b]From Cheng and Navrotsky [23].
[c]Uncertainty is two standard deviations of the mean, number in ( ) is the number of experiments.

dopant ions. Energetic parameters for these defect formation reactions are derived from calorimetric data.

3.3. Enthalpy of oxidation

DS calorimetry of samples with constant doping content, x, and varying oxygen deficiency, δ, is used to determine the enthalpy of oxidation. For all samples we adopt the point defect model assuming the formal valence states of Cr would be 3+ and/or 4+ and without implying any microscopic picture of partial oxidation state, band occupancy, or covalency. Thus, the enthalpy of oxidation (ΔH_{oxid}) between two samples is determined by the thermochemical cycle shown in

Table 4
Thermochemical cycle for calculation of the enthalpy of oxidation (ΔH_{oxid}) between two $La_{1-x}A_xCrO_{3-\delta}$ samples (A = Ca or Sr) which only differ in oxygen contents (assuming $\delta' > \delta$).

Reaction	ΔH
$La_{1-x}A_xCrO_{3-\delta'}(xl, 298\,K) \rightarrow 0.5(1-x)La_2O_3(sol, 1080\,K) + 0.5\,Cr_2O_3(sol, 1080\,K) + x\,AO(sol, 1080\,K) + (0.25x - 0.5\delta')\,O_2(g, 1080\,K)$	$\Delta H(10) = \Delta H_{DS}(La_{1-x}A_xCrO_{3-\delta'})$
$La_{1-x}A_xCrO_{3-\delta}(xl, 298\,K) \rightarrow 0.5(1-x)La_2O_3(sol, 1080\,K) + 0.5\,Cr_2O_3(sol, 1080\,K) + x\,AO(sol, 1080\,K) + (0.25x - 0.5\delta)\,O_2(g, 1080\,K)$	$\Delta H(11) = \Delta H_{DS}(La_{1-x}A_xCrO_{3-\delta})$
$O_2(g, 298\,K) \rightarrow O_2(g, 1080\,K)$	$\Delta H(7) = \Delta H_{298-1080}(O_2)$
$La_{1-x}A_xCrO_{3-\delta'}(xl, 298\,K) + 0.5(\delta'-\delta)\,O_2(g, 298\,K) \rightarrow La_{1-x}A_xCrO_{3-\delta}(xl, 298\,K)$	$\Delta H(12) = \Delta H_{oxid}$ from $3-\delta'$ to $3-\delta$
$\Delta H(12) = \Delta H(10) - \Delta H(11) + 0.5(\delta'-\delta)\,\Delta H(7)$	

Table 4 and represents the enthalpy change of the reaction:

$$La_{1-x}A_xCrO_{3-\delta'}(xl,\ 298\,K) + 0.5(\delta' - \delta)O_2(g,\ 298\,K) \rightarrow La_{1-x}A_xCrO_{3-\delta}(xl,\ 298\,K). \quad (3)$$

The defect chemistry can be written as the inverse of Eq. (2):

$$2Cr_{Cr}^{x} + V_O^{\cdot\cdot} + 0.5O_2(g) = 2Cr_{Cr}^{\cdot} + O_O^{x}. \quad (4)$$

One example is the oxidation of L20SC2.91 to L20SC3.0. The heat of oxidation is calculated as -15.78 ± 2.62 kJ/mol using their enthalpies of DS and the correction for the heat content of oxygen (Table 4). This is actually the difference between the enthalpies of formation of L20SC3.0 and L20SC2.91 at room temperature. This value is in good agreement with that obtained from the DSC measurement in Fig. 1(c), i.e., the area under the DSC peak, -15.49 ± 1.40 kJ/mol. The heats of oxidation for L10SC and L30CC determined by DS calorimetry are -8.73 ± 3.04 and -12.42 ± 2.77 kJ/mol, respectively, which also agree reasonably with those from DSC measurements (Fig. 1(b) and (d)). One might argue that using DSC to measure the enthalpy of oxidation would be more direct and accurate. However, careful examination of the TG/DSC curves indicates that oxygen absorption occurs quickly at 300–700 K but is incomplete by 700 K. Slow but steady oxygen gain continues from 700 to 1173 K (Fig. 1(b) to (d)) and during the 1173 K isotherm for 1 h. So the DSC peak is not adequate to represent the total enthalpy of oxidation. The slow gain occurring at 1173 K also precludes accurate measurement by transposed temperature drop calorimetry at 298–1173 K, due to the long reaction time. Therefore, DS calorimetry is the only clean technique to directly determine the enthalpy of oxidation. For convenience, ΔH_{oxid} is normalized to kJ/mol O_2.

The enthalpy of oxidation (reaction (3)) could be a function of doping amount (x) and oxygen deficiency (δ). However, many studies, including doped manganite [21] and ferrite perovskite systems [22], have shown that the enthalpy of formation from oxides is a good linear function of the oxygen content, implying that the enthalpy of oxidation in each series of a given dopant composition is virtually independent of the degree of oxygen nonstoichiometry. Available data in this study are insufficient to test the linearity of $\Delta H_{f,ox}$ vs. δ since there are only two samples in each series. Nevertheless, as a first approximation, the enthalpy of oxidation between two samples is taken as that for the whole series. For instance, ΔH_{oxid} in 20% Sr-doped $LaCrO_3$ is -351 ± 58 kJ/mol O_2.

The enthalpies of oxidation, along with the data available in the literature [3,4,12,14], are plotted vs. dopant composition (x) in Fig. 2(a) and (b) for Ca- and Sr-doped systems, respectively. The uncertainty of each data point reflects the standard deviation of the calorimetric measurements and is relatively large. The uncertainty is magnified because the difference in the enthalpy of formation of samples with the same x but different δ is small, and the difference in oxygen content ($\delta'-\delta$) is also small. The values of ΔH_{oxid} in the Ca-doped system (Fig. 2(a)) overlap with those in the Sr-doped counterparts (Fig. 2(b)) and the difference caused by the nature of divalent cations (Ca vs. Sr) cannot be resolved.

The ΔH_{oxid} data in both Ca- and Sr-doped systems are in excellent agreement with the literature data for $x = 0.1$, but are somewhat more endothermic for $x = 0.2$ and 0.3. It would be an overinterpretation to attempt to compare the absolute values of the current calorimetric data sets with others, because assumptions and approximations differ in each study, the temperature range in which each experiment was conducted varies, and the uncertainties are unknown in some cases. The salient point, however, is that the enthalpy of oxidation tends to change in the endothermic direction with increasing doping amount in both Ca- and Sr-doped cases. This may relate to the chemical nature of Ca and Sr that accept a lower oxygen coordination state more

readily than the host La. Furthermore, we argue that this is a strong indication of short-range ordering between dopants and oxygen vacancies (see next section).

A comparison of the enthalpy of oxidation in Sr-doped $LaCrO_3$ (LSC), $LaMnO_3$ (LSM), and $LaFeO_3$ (LSF) systems (Table 5) gives some insight on their applications in SOFCs as different components. The enthalpy of oxidation in the chromite system is about -400 kJ/mol O_2 (this study) and that in the manganite system is about -700 kJ/mol O_2 [21]. Both are much more exothermic than those in the ferrite system, -200 kJ/mol O_2 [22]. Under the same conditions, LSC and LSM materials would be more resistant to oxygen reduction than LSF. For example, at the cathode side when an SOFC is running at 1273 K, LSC and LSM do not lose oxygen and show exclusive electronic conduction, while LSF is partially reduced, which makes it a mixed ionic and electronic conductor. Thus LSF perovskites are currently studied as new cathode materials to replace the conventional LSM [32], because the reaction zone of oxygen reduction is extended from the triple-phase boundary (where oxygen gas, cathode and electrolyte meet) to the entire cathode surface. The calorimetric data support such application.

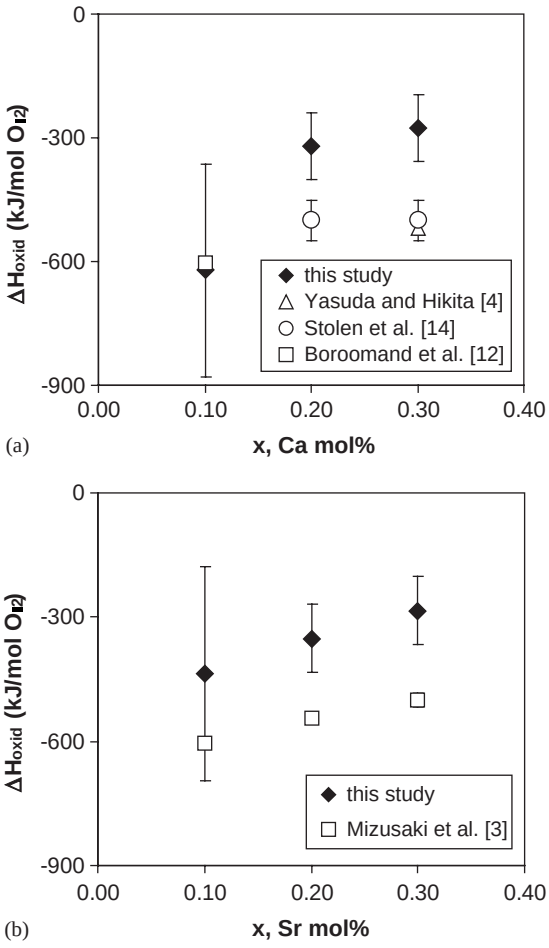

Fig. 2. Enthalpy of oxidation (ΔH_{oxid}, in kJ/mol O_2) as a function of dopant composition in the system of (a) $La_{1-x}Ca_xCrO_{3-\delta}$, and (b) in the $La_{1-x}Sr_xCrO_{3-\delta}$. Data from literature studies are also included for comparison [3,4,12,14].

3.4. Oxygen vacancy ordering in $La_{1-x}A_xCrO_{3-\delta}$ ($\delta > 0$)

As shown in Fig. 2, the enthalpy of oxidation in both Ca- and Sr-doped systems becomes more endothermic with increasing doping. Bearing in mind that the oxidation of Cr^{3+} to Cr^{4+} is accompanied by the filling of oxygen vacancies (Eq. (4)), a more endothermic enthalpy of oxidation implies a stronger tendency to retain oxygen vacancies. This suggests that, in oxygen-deficient chromite perovskites, oxygen vacancies may be stabilized by some means such as short-range ordering. Thus oxygen vacancies are not randomly distributed. Mizusaki et al. [3] used TG to investigate the thermodynamics in the LSC system in which ΔH_{oxid} was found to be a function of Sr content (Fig. 2(b)). The dependence is ascribed to the strong interaction between strontium and the oxygen sublattice [3]. Sakai et al. [28] studied the crystal structure of the reduced L20CC with powder neutron diffraction and the structure refinement indicates that oxygen vacancies are preferentially located at the planar oxygen sites over the apical ones. The effect of short-range vacancy ordering on the enthalpy of oxidation is also observed in the Sr-doped $LaFeO_3$ system [22].

On the other hand, ideal solution models have been proposed in the literature [14,33]. Stølen et al. [14]

Table 5
Enthalpy of vacancy formation and enthalpy of oxidation for Sr-doped $LaCrO_3$, $LaMnO_3$, $LaFeO_3$, and La_2CuO_4 systems

System	Doping range	Enthalpy of vacancy formation		Enthalpy of oxidation (kJ/mol of O_2)	Reference
		(kJ/mol of $V_O^{\cdot\cdot}$)	(kJ/mol of O_2)		
$La_{1-x}Sr_xCrO_{3-\delta}$	$0<x\leqslant 0.3$	395 ± 30	790 ± 60	$-510+760x$[a] (Cr^{3+} to Cr^{4+})	This study
$La_{1-x}Sr_xMnO_{3-\delta}$	$0<x\leqslant 0.5$	383 ± 24	766 ± 48	-740 ± 10 (Mn^{3+} to Mn^{4+})	Laberty et al. [21]
$La_{1-x}Sr_xFeO_{3-\delta}$	$0<x\leqslant 0.5$	90 ± 11	180 ± 22	-200 ± 50 (Fe^{3+} to Fe^{4+})	Cheng et al. [22]
$La_{2-x}Sr_xCuO_{4-\delta}$	$0<x\leqslant 1.0$	0 ± 10	0 ± 20	-130 ± 20 (Cu^{2+} to Cu^{3+})	Bularzik et al. [18]

[a]The enthalpy of oxidation in Sr-doped $LaCrO_3$ system is approximately a linear function of the dopant composition.

observed nearly constant enthalpies of oxidation for 20% and 30% doped $LaCrO_3$ (Fig. 2(a)) and suggested a random distribution of defects. Yasuda and Hishinuma [33] studied the chemical diffusion in reduced LCC samples and concluded that oxygen vacancies were not interacting since the oxygen vacancy diffusion coefficient was independent of the vacancy concentration. To resolve these differences, more work on crystal chemistry is needed, such as high-resolution neutron diffraction and transmission electron microscopy.

3.5. Energetic trends in $La_{1-x}A_xCrO_3$

Enthalpies of formation from oxides for fully oxidized chromite samples, along with the $\Delta H_{f,ox}$ of the end-member $LaCrO_3$ [23], are plotted vs. dopant concentration in Fig. 3. In both Ca- and Sr-doped perovskites, the formation enthalpy changes strongly with the dopant concentrations, becoming more endothermic with increasing alkaline earth substitution. This trend is in sharp contrast to the Sr-doped ferrite system [22] in which the enthalpy of formation is practically independent of Sr content at $x = 0-0.5$, and to the Sr-doped manganite system [21] in which the enthalpies of formation of doped samples are only slightly more endothermic than for undoped $LaMnO_3$.

To understand these differences, we take the following approach using Sr-doped perovskites as well as perovskite-related La_2CuO_4 (K_2NiF_4-type) as examples. The formation of fully oxidized $La_{1-x}Sr_xCrO_3$ may be conceptually separated into two steps:

$$(1-x)La_2O_3 + xSrO + Cr_2O_3 = La_{1-x}Sr_xCrO_{3-x/2}, \quad (5)$$

$$La_{1-x}Sr_xCrO_{3-x/2} + 0.25xO_2 = La_{1-x}Sr_xCrO_3. \quad (6)$$

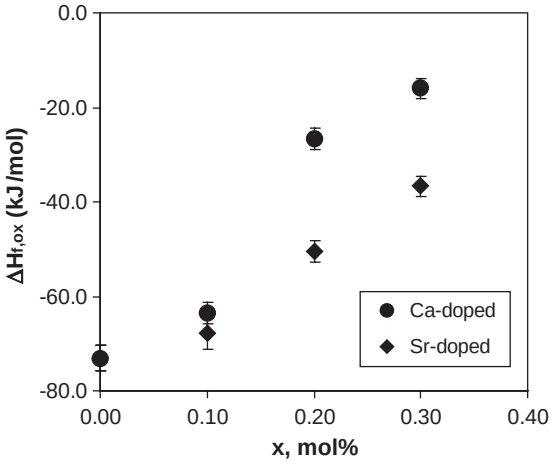

Fig. 3. Enthalpies of formation from oxides for the $La_{1-x}A_xCrO_3$ solid solutions vs. dopant concentration.

Reaction (5) incorporates the coupled substitution

$$Sr_{Sr}^{x} + O_O^{x} = Sr_{La}^{'} + 0.5V_O^{\cdot\cdot} + 0.5O_2 \quad (7)$$

and does not involve any oxidation. Reaction (6) is the oxidation to the fully oxidized state and the defect chemistry is represented by Eq. (4). Since the enthalpy of formation for a series with a given dopant concentration is assumed to vary linearly with oxygen nonstoichiometry (δ), enthalpies of formation for the maximally reduced samples (enthalpy change for reaction (5)) can be extrapolated from the plots of $\Delta H_{f,ox}$ vs. δ. Enthalpies of formation for the fully oxidized samples were directly determined from our calorimetric measurements. We plot the enthalpies of formation for maximally reduced and fully oxidized Sr-doped $LaCrO_3$ samples vs. Sr content in Fig. 4(a) and (b), respectively. Also plotted are the formation enthalpy data for Sr-doped $LaMnO_3$ [21], $LaFeO_3$ [22], and La_2CuO_4 [18] for comparison.

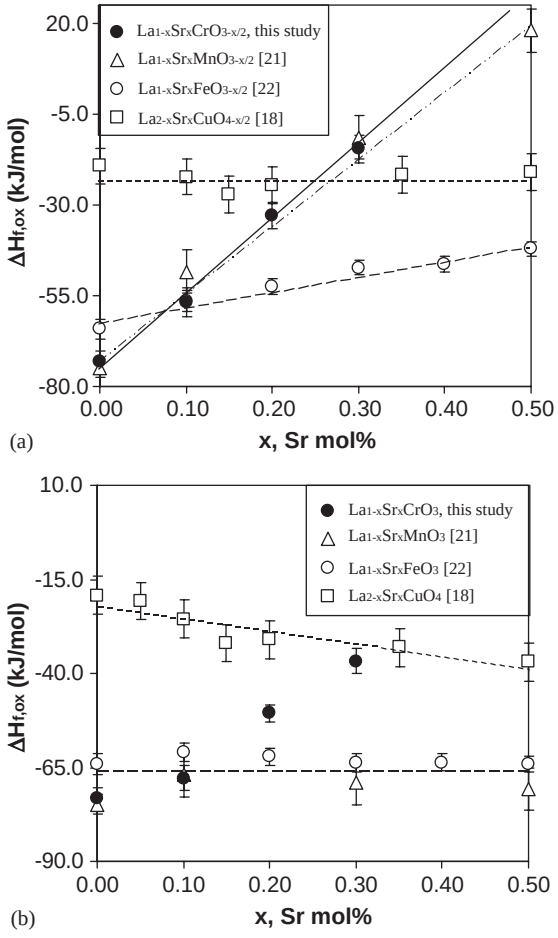

Fig. 4. Enthalpies of formation from oxides vs. Sr content for Sr-doped $LaCrO_3$ (this study), $LaMnO_3$ [21], $LaFeO_3$ [22], and La_2CuO_4 [18] systems. (a) Maximally reduced samples. Enthalpy of vacancy formation is calculated for each system. (b) Fully oxidized samples. The energetic trend in each system is controlled by the enthalpy of vacancy formation and the enthalpy of oxidation. Lines are the linear fits for each system.

As seen in Fig. 4(a), for each system that is maximally reduced, the enthalpies of formation are approximately linear functions of Sr content (x) or oxygen deficiency (δ) since $\delta = 0.5x$. Similar to the doped $LaGaO_3$ systems [29], the slope of each fitted line represents the enthalpy of charge-coupled substitution involving oxygen vacancy formation. For brevity, the short term "enthalpy of vacancy formation" is used for the enthalpy of this reaction (Eq. (5)) and its value is often normalized to kJ/mol of $V_O^{\cdot\cdot}$. Values of enthalpy of vacancy formation for each system, along with the values of enthalpy of oxidation, are summarized in Table 5. To enable the direct comparison between these two parameters, the enthalpy of vacancy formation is also expressed in terms of kJ/mol of O_2 by multiplying by a factor of 2.

There is a rapid change in the enthalpy of vacancy formation along the first row of transition metals (in the order Cr, Mn, Fe, Cu). The enthalpy decreases from a large endothermic value of 790 ± 58 kJ/mol O_2 for chromites to essentially zero for cuprites. This suggests that oxygen vacancies become easier to form in that order. The energetic trends in the fully oxidized systems (Fig. 4(b)) result from the competition between the enthalpy of vacancy formation and the enthalpy of oxidation. In the perovskite-related $La_{2-x}Sr_xCuO_4$ solid solution [18], the heat effect from oxygen vacancy formation is almost zero, so oxidation is effectively the main factor influencing the composition dependence of the enthalpy of formation, which linearly becomes more exothermic with a slope equal to the enthalpy of oxidation (-130 ± 20 kJ/mol O_2). The enthalpies of vacancy formation in both the ferrite system [22] and the manganite system [18] are comparable in magnitude to the enthalpies of oxidation (Table 5), so they are almost canceled out and the enthalpy of formation is virtually independent of Sr content (Fig. 4(b)). For the fully oxidized LSC perovskites, enthalpies of formation become more endothermic with increasing doping (Fig. 4(b)). This is because of the extremely endothermic enthalpy of vacancy formation that dominates the exothermic enthalpy of oxidation (Table 5).

Also seen in Fig. 3 is the general trend that, at a given composition, an Sr-doped sample is more stable than a Ca-doped one. This is understandable because increasing basicity of the A-site divalent cation (Sr vs. Ca) more strongly stabilizes the high oxidation state of chromium on the B-site, as has been observed in other perovskite-related systems [19,21].

4. Conclusions

Oxygen nonstoichiometry (δ) in Ca- and Sr-doped $LaCrO_3$ perovskites is a function of the doping amount, oxygen partial pressure, and annealing temperature. Samples prepared in air or O_2 are fully oxidized. Reduced samples with appreciable amount of oxygen deficiency were obtained when treated in a reducing atmosphere (1% H_2 + 99% Ar) at 1273 K for 1 h. High-temperature DS calorimetry was performed to determine the enthalpy of formation from oxides for each sample. Enthalpy of oxidation in both Ca- and Sr-doped systems is assumed independent of oxygen nonstoichiometry (δ) but varies with dopant concentration (x). With increasing doping, the enthalpy of oxidation becomes more endothermic, implying that short-range oxygen vacancy ordering exists in the reduced samples. In fully oxidized systems where the charge difference is all compensated by the oxidation of Cr^{3+} to formal Cr^{4+}, the enthalpy of formation is a function of composition and controlled by the enthalpy of oxygen vacancy formation and the enthalpy of oxidation. The large endothermic enthalpy of vacancy formation causes the enthalpy of formation to become more endothermic with increasing doping in both Ca- and Sr-doped $LaCrO_3$ systems.

Though the difference in the enthalpy of oxidation between Ca and Sr doping (Fig. 2) is not obvious, the enthalpies of formation from oxides (Fig. 3) confirm that more basic A-site divalent cation (Sr vs. Ca) energetically stabilizes the high oxidation state of B-site cation in chromite perovskites.

Acknowledgments

The authors thank S. Roeske for help with the electron microprobe analysis. This project was supported by the US Department of Energy (DOE) (Grant No. DEFG03–97ER45654).

References

[1] N.Q. Minh, J. Am. Ceram. Soc. 76 (1993) 563.
[2] M. Mori, T. Yamamoto, H. Itoh, T. Watanabe, J. Mater. Sci. 32 (1997) 2423.
[3] J. Mizusaki, S. Yamauchi, K. Fueki, A. Ishikawa, Solid State Ionics 12 (1984) 119.
[4] I. Yasuda, T. Hikita, J. Electrochem. Soc. 140 (1993) 1699.
[5] A. Zuev, L. Singheiser, K. Hilpert, Solid State Ionics 147 (2002) 1.
[6] F.A. Kröger, The chemistry of imperfect crystals, vol. 1–3, North-Holland, Amsterdam, 1974.
[7] D.P. Karim, A.T. Aldred, Phys. Rev. B 20 (1979) 2255.
[8] H.U. Anderson, Mater. Sci. Res. 11 (1978) 469.
[9] N.Q. Minh, C.R. Horne, F.S. Liu, D.M. Moffatt, P.R. Staszak, T.L. Stillwagon, J.J. Van Ackeren, Proceedings of the 25th Intersociety Energy Conversion Engineering Conference, vol. 3, American Institute of Chemical Engineers, New York, 1990, pp. 230–234.
[10] K. Oikawa, T. Kamiyama, T. Hashimoto, Y. Shimojyo, Y. Morii, J. Solid State Chem. 154 (2000) 524.
[11] H. Hayashi, M. Watanabe, M. Ohuchida, H. Inaba, Y. Hiei, T. Yamamoto, M. Mori, Solid State Ionics 144 (2001) 301.

[12] F. Boroomand, E. Wessel, H. Bausinger, K. Hilpert, Solid State Ionics 129 (2000) 251.
[13] T.R. Armstrong, J.W. Stevenson, L.R. Pederson, P.E. Raney, J. Electrochem. Soc. 143 (1996) 2919.
[14] S. Stølen, N. Sakai, E. Bakken, J. Therm. Anal. Calorimetry 57 (1999) 823.
[15] S. Stølen, J. Chem. Thermodyn. 30 (1998) 1495.
[16] A. Navrotsky, Phys. Chem. Miner. 2 (1977) 89.
[17] A. Navrotsky, Phys. Chem. Miner. 24 (1997) 222.
[18] J. Bularzik, A. Navrotsky, J. DiCarlo, J. Bringley, B. Scott, S. Trail, J. Solid State Chem. 94 (1991) 418.
[19] J. DiCarko, J. Bularzik, A. Navrotsky, J. Solid State Chem. 96 (1992) 381.
[20] A. Navrotsky, Pure Appl. Chem. 66 (1994) 1759.
[21] C. Laberty, A. Navrotsky, C.N.R. Rao, P. Alphonse, J. Solid State Chem. 145 (1999) 77.
[22] J. Cheng, A. Navrotsky, X.-D. Zhou, H.U. Anderson, Thermochemistry of $La_{1-x}Sr_xFeO_{3-\delta}$ solid solutions ($0.0 \leqslant x \leqslant 1.0$, and $0.0 \leqslant \delta \leqslant 0.5$), Submitted.
[23] J. Cheng, A. Navrotsky, X.-D. Zhou, H.U. Anderson, Enthalpies of formation of $LaMO_3$ perovskite (M = Cr, Fe, Co and Ni), J. Mater. Res., in press.
[24] C.P. Khattak, D.E. Cox, Mater. Res. Bull. 12 (1977) 463.
[25] M. Mori, T. Yamamoto, T. Ichikawa, Y. Takeda, Solid State Ionics 148 (2002) 93.
[26] R.A. Robie, B.S. Hemingway, Thermodynamic properties of minerals and related substances at 298.15 K and 1 Bar (10^5 Pascals) pressure and at higher temperatures, US Geological Survey Bulletin No. 2131, Washington, DC, 1995.
[27] N. Sakai, S. Stølen, J. Chem. Thermodyn. 28 (1996) 421.
[28] N. Sakai, H. Fjellvåg, B.C. Hauback, J. Solid State Chem. 121 (1996) 202.
[29] J. Cheng, A. Navrotsky, J. Solid State. Chem. 177 (2004) 126.
[30] J. Cheng, A. Navrotsky, J. Mater. Res. 18 (2003) 2501.
[31] R.D. Shannon, Acta Crystallogr. A 32 (1976) 751.
[32] K. Huang, H.Y. Lee, J.B. Goodenough, J. Electrochem. Soc. 145 (1998) 3220.
[33] I. Yasuda, M. Hishinuma, J. Solid State Chem. 115 (1995) 152.